A Dual Functional Solid Liquid Separation Process Based on Filtration and Settling

The dual functional filter combines both the mechanisms of filtration and settling or decantation. The combined mechanisms of separation permit very high degrees of sludge dewatering; for example, slurries containing 0.2 wt. % gelatinous particles have been dewatered to produce a sludge of 35 wt. % particles. A mathematical model which includes both the effects of axial (vertical) variation of pressure driving force and cake compressibility effects is used in conjunction with experimental data to evaluate the dual functional filter performance.

JOSEPH D. HENRY, JR.
ALAIN P. LUI
and
C. H. KUO

Department of Chemical Engineering
West Virginia University
Morgantown, West Virginia 26506

SCOPE

The dual functional filter is a solid-liquid separation process which employs both the mechanisms of filtration and settling. The process has the potential for dewatering slurries of micron sized gelatinous materials that are difficult to dewater by other methods. The dual functional filter utilizes vertical, collapsible, porous hoses as a filtration medium. The pressure driving force in this device is a function of the axial (vertical) position along the hose. There have been no previous theoretical interpretations of performance data for a dual functional filter. A mathematical model was developed which includes both the axial or vertical variation of the pressure driving force and cake compressibility effects. Related mathematical models have been published by Tiller (1972) and by Holland and Woodham (1956) which include the variations in pressure driving force due to hydrostatic head for a rotary vacuum filter. Both of these models were developed for the case of constant cake resistance. The model which includes both cake compressibility and pressure driving force variation was used to interpret experimental performance data for slurries of neutralized acid mine drainage sludge. These slurries involve particles which are highly gelatinous and provide a severe test of the filter performance and the applicability of the mathematical model to the case of a highly compressible filter cake.

CONCLUSIONS AND SIGNIFICANCE

The performance of sludge dewatering processes which employ conventional filtration is often limited by both the degree of dewatering that can be attained and a low filtration rate. This is the usual case when slurries of micron sized gelatinous particles are being dewatered. A novel filtration process is discussed here which offers a solution to both of these problems. The dual functional filter combines both the mechanisms of filtration and settling.

A dual functional filter was constructed and operated which can determine the filtration rate as a function of axial position along the hose. This permits direct observation of the influence of the variable pressure driving force at various positions along the filter hose. A mathematical model was developed to describe the performance of the dual functional filter. There have been no previous attempts to model this filter. The model includes the effects of both the axial variation of the pressure driving force and filter cake compressibility. The filtration rate data for neutralized acid mine water sludge are consistent with the assumption that cake resistance is a power function of the applied pressure. The model predicts the experimental data with a maximum deviation of $\pm 15\%$.

Filter cakes formed from lime neutralized acid mine sludge are compressible; for example, at a feed concentration of 0.2 wt. %, the specific cake resistance is proportional to $\Delta P^{0.5}$ for pressures above 2.1 kN/m^2. The exponent in this relation would be zero for a perfectly incompressible cake. The filtration rate increases slowly with pressure above 40 kN/m^2. The model contains three empirical parameters: the coefficient of specific cake resistance a, the compressibility factor n, and the empirical pressure constant ΔP_i, which are evaluated from data.

The dual functional nature of the process provides a very high degree of sludge dewatering. Filtration combined with settling produces sludge of 35 wt. %* solids from a feed with 0.2 wt. % solids. This coupled with the high filtration rates attained by rapid cyclic operation of the filter justifies its consideration as an alternative solid-liquid separation process for micron sized gelatinous particles.

DUAL FUNCTIONAL FILTER CONCEPT

The dual functional filter employs the mechanisms of filtration and settling. These two distinct mechanisms of separation are obtained by using a filter constructed with a vertical collapsible porous hose, illustrated schematically in Figure 1. The filtration cycle consists of three phases: a filtration phase, a dump phase, and a settling phase.

The filtration phase of the cycle is conducted with slurry introduction at the top and a valve closed at the bottom of the hose. The filter cake accumulates on the interior wall of the hose. Filtrate is removed through

Correspondence concerning this paper should be addressed to Joseph D. Henry, Jr.

* Volume percent solids are not reported because many different types of particles are present. The voidage and average specific gravity were not measured.

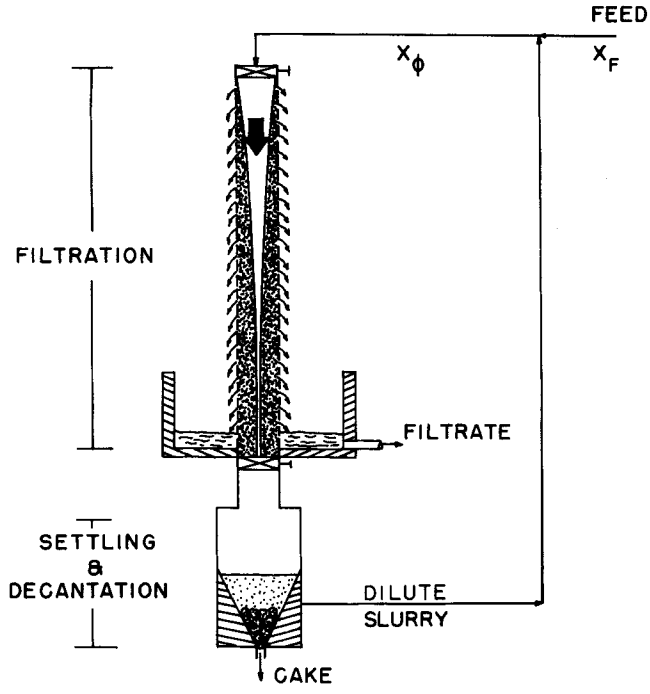

Fig. 1. Dual functional filter.

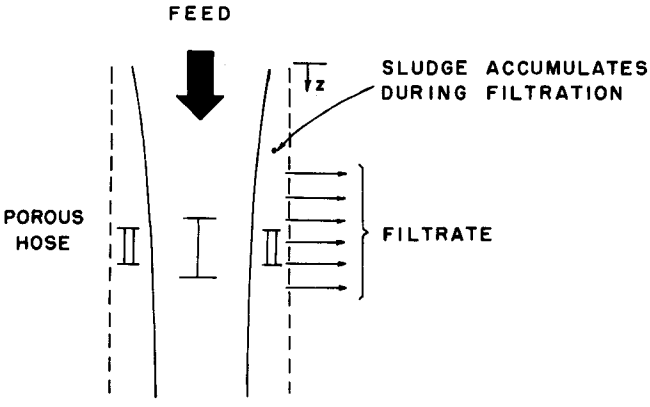

Fig. 2. Slurry and cake regions within the filter.

the porous wall of the hose. The filtration phase of the cycle is terminated before the solids fill the hose.

The dump phase of the cycle is initiated by closing the feed valve at the top of the hose and by opening the valve at the bottom of the hose. The resulting pressure shock causes the cake and feed slurry in the vertical hose to dump to a receiver. This heterogeneous material is composed of cake and a dilute slurry; that is, the cake does not redisperse completely into the interior core of feed liquid.

The third phase of the cycle consists of settling the cake that is dumped to the receiver. This heterogeneous mixture is ideally suited for effective settling and decantation. The decanted slurry has a particle concentration equal to or greater than the feed concentration. This occurs owing to the possible redispersion of a portion of the filter cake into the interior core of feed liquid during dumping.

The dual functional filter provides several process advantages over conventional filtration processes:

1. The rapid cyclic nature of the process produces very high filtration rates; that is, the filtration cake is not allowed to accumulate to a large thickness.
2. There is no mechanical device required for cake removal from the filter hose.
3. The combination of the filtration and settling mechanisms allows very high degrees of sludge dewatering compared to other processes.
4. Filter aid is not generally required.
5. The simplicity of this filter, that is, the absence of moving parts or vacuum equipment, should promote its commercial development.

PREVIOUS WORK

There are extremely limited performance data for the dual functional filter in the literature. The filter was invented by Popper and Camirand (1970). Their patent refers to the device as a Uni-Flow Filter. Page, et al., (1972) have obtained sludge concentrations in excess of 25 wt. % solids with 0.1 wt. % solids in neutralized acid mine drainage sludges. Investigators at Hittman Associates (1974) have found that flexible porous polypropylene hoses offer superior cake dumping characteristics to hoses constructed, for example, from dacron. No previous attempts have been made to model the performance of a dual functional filter.

In view of the minimal information available on the performance of the dual functional filter, a mathematical model and appropriate experimental data are critical to evaluate the filter performance and provide a basis for design. The model which includes both the effects of variation of pressure driving force and cake compressibility will be utilized. A related model which considers the effect of variations in pressure driving force due to hydrostatic head and rotary vacuum filters has been presented by Tiller (1972) and by Holland and Woodham (1956). Neither of these investigators considered the simultaneous effect of variation in pressure driving force and cake compressibility.

Other filters have employed a vertical filter medium where the pressure driving force is a function of axial position along the medium. The Guva tower belt filter (manufactured by Prefiltec AG & Miura Chemical E. Co.) and the Winklepress are examples. The model for the filtration phase of the cycle developed here could be modified and applied to these filters. The dump phase of both these filters is more complicated than that of the dual functional filter. In both cases these filters use mechanical means, such as conveyor belts, to recover the filter cake.

THEORY

A mathematical model is developed for the filtration phase of the operating cycle of the dual functional filter. The model includes both the effects of axial (vertical) variation of the pressure driving force and filter cake compressibility. The primary goal is to obtain expressions that relate both the filtration rate and cake thickness to axial position along the hose and time.

Owing to the pressure variation along the hose, the cake is thicker at the bottom of the hose than at the top. Two regions, I and II, are defined for the slurry and cake phases respectively and are illustrated in Figure 2. The cake particles are assumed not to redisperse into region I during the filtration phase of the cycle; that is, once a particle enters the cake it stays there. This is a reasonable assumption in view of the very low shear stress between the surface of the cake and the region I liquid.

Rate Law

Ruth (1946) has developed an expression for the relationship between the filtration flux, applied filtration pressure, and average specific cake resistance:

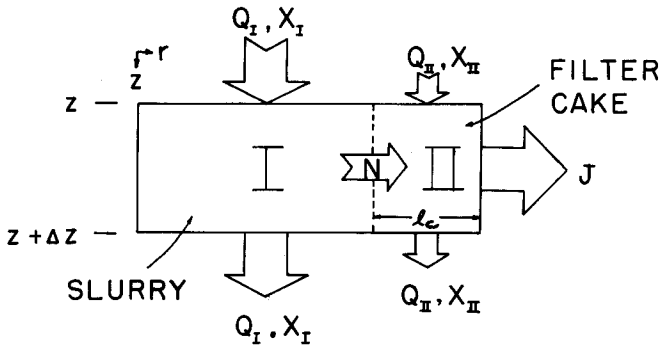

Fig. 3. Relationship of variables for the mathematical model.

$$J = \frac{\rho_v}{\mu(\alpha_{avg}\omega + R_m)}\Delta P \quad \text{where} \quad \omega = X_{II}\rho_{II}l_c \qquad (1)$$

Owing to the high porosity thin filter media (hoses) that are employed, the filter medium resistance can be neglected relative to that of the gelatinous, compressible filter cake. Neglecting the medium resistance, Equation (1) becomes

$$J = \frac{\rho_v}{\mu\alpha_{avg}\omega}\Delta P \qquad (2)$$

Tiller (1962) and others have shown that most experimental data are consistent with the specific cake resistance-pressure dependence as follows:

$$\alpha = a\Delta P^n \qquad \text{where} \quad \Delta P > \Delta P_i \qquad (3)$$

$$\alpha = \alpha_i = a\Delta P_i^n \qquad \text{where} \quad \Delta P \leq \Delta P_i \qquad (4)$$

To obtain the average specific cake resistance, local values must be integrated across the cake:

$$\frac{1}{\alpha_{avg}} = \frac{1}{\Delta P}\int_0^{\Delta P}\frac{1}{\alpha}d(\Delta P)$$

$$= \frac{1}{\Delta P}\left[\int_0^{\Delta P_i}\frac{d(\Delta P)}{\alpha_i} + \int_{\Delta P_i}^{\Delta P}\frac{d(\Delta P)}{a\Delta P^n}\right] \qquad (5)$$

$$\alpha_{avg} = \frac{a(1-n)\Delta P}{\Delta P^{1-n} - n\Delta P_i^{1-n}} = \frac{a(1-n)\Delta P^n}{1 - n(\Delta P_i/\Delta P)^{1-n}} \qquad (6)$$

This expression will be used in conjunction with the model that is developed below.

Formulation of Model

The mathematical model developed below utilizes differential material balances for slurry and solid particles in both regions I and II. The dependence of the cake thickness l_c and the filtration flux J on time and axial position are obtained by applying an appropriate form of the Ruth equation to the resulting differential equations.

The partial differential equations which describe the filtration phase of the cycle are developed in full generality prior to applying the assumptions. This is done to emphasize the several assumptions employed which do not arise in conventional batch filtration theory because there is a negligible pressure gradient parallel to the filter surface.

The internal flows are shown in relation to a differential element in Figure 3. Overall and particle material balances can be made on both the slurry region (I) and the cake region (II) to give partial differential equations that describe the behavior of the filter.

Total material balances:

Region I

$$\frac{\partial Q_I}{\partial Z} + 2\pi rN + \frac{\partial}{\partial t}(\pi r^2\rho_I) = 0 \qquad (7)$$

Region II

$$\frac{\partial Q_{II}}{\partial Z} + 2\pi RJ - 2\pi rN + \frac{\partial}{\partial t}[\pi(R^2 - r^2)\rho_{II}] = 0 \qquad (8)$$

Solid particle balances:

Region I

$$\frac{\partial}{\partial Z}(X_IQ_I) + 2\pi rX_IN + \frac{\partial}{\partial t}(\pi r^2\rho_IX_I) = 0 \qquad (9)$$

Region II

$$\frac{\partial}{\partial Z}(X_{II}Q_{II}) + 2\pi RX_vJ - 2\pi rX_IN + \frac{\partial}{\partial t}[\pi(R^2 - r^2)X_{II}\rho_{II}] = 0 \qquad (10)$$

The following assumptions are included in the model:

1. The filter hose used as filter medium is so porous and thin that the medium resistance is negligible.
2. The axial flow of slurry through the cake region (Q_{II}) is small compared to that through the slurry feed region (Q_I).
3. The solid concentration of cake X_{II} is much larger than that of slurry feed X_I, that is, $X_{II} >> X_I$. These two concentrations are assumed to be independent of Z and t.
4. There is no breakthrough of particles through the medium, that is, $X_v \simeq 0$.
5. The cake thickness l_c is much smaller than the diameter of the filter hose, that is, $l_c << 2R$; therefore, $r^2 \simeq R^2 - 2Rl_c$.
6. The pressure along the filter hose is linearly dependent on Z ($\Delta P(Z) = \Delta P_0 + \rho_I g\Delta Z$).
7. Radial variations in each region are negligible.
8. All physical properties are assumed to be constant.

Assumption 5 states that the cake thickness l_c is much smaller than the diameter of the filter hose, that is, $r^2 \simeq R^2 - 2Rl_c$. This assumption and assumptions 2 and 4 can be used to simplify the material balances, Equations (7) to (10). This is done by subtracting the sum of Equations (9) and (10) from the sum of Equations (7) and (8) multiplied by X_I to obtain

$$X_IJ + (X_I - X_{II})\rho_{II}\frac{\partial l_c}{\partial t} = 0 \qquad (11)$$

It is noted that the solid concentration of the cake (region II) is 150 to 300 times the solid concentration of the feed slurry (region I). Assumption 3 ($X_{II} >> X_I$) can therefore be used to simplify Equation (11):

$$X_IJ = X_{II}\rho_{II}\frac{\partial l_c}{\partial t} = \frac{\partial \omega}{\partial t} \qquad (12)$$

This is the conventional batch filtration material balance equation. The discussion of the partial differential material balances and related assumptions justifies the application of the batch filtration equation with an axial varying pressure driving force to the dual functional filter. The details of the mathematical model have been discussed by Lui (1974).

The Ruth equation as shown in Equation (2) is then substituted into Equation (12):

$$\omega d\omega = \frac{X_I \rho_v \Delta P}{\mu \alpha_{avg}} dt \tag{13}$$

Since $\omega = 0$ at $t = 0$, Equation (13) is integrated to obtain the amount of dry cake per unit area ω:

$$\omega = \sqrt{\frac{2X_I\rho_v\Delta P}{\mu\alpha_{avg}}}\, t = \sqrt{\frac{2X_I\rho_v t}{\mu a(1-n)}}\,[\Delta P^{1-n} - n\Delta P_i^{1-n}]^{1/2} \tag{14}$$

The cake thickness l_c can be obtained from Equation (14):

$$l_c = \frac{\omega}{X_{II}\rho_{II}} = \frac{1}{X_{II}\rho_{II}} \sqrt{\frac{2X_I\rho_v t}{\mu a(1-n)}}\,[\Delta P^{1-n} - n\Delta P_i^{1-n}]^{1/2} \tag{15}$$

Substituting Equation (14) into the Ruth equation with R_m negligible [Equation (2)], we obtain the differential filtration flux J:

$$J = \sqrt{\frac{\rho_v}{2\mu a(1-n)X_I t}}\,[\Delta P^{1-n} - n\Delta P_i^{1-n}]^{1/2} \tag{16}$$

The measurable filtration flux W' over a hose segment $Z_2 - Z_1$ is defined as

$$W' = \frac{1}{(Z_2 - Z_1)} \int_{Z_1}^{Z_2} J\, dZ \tag{17}$$

Equation (16) is expanded by Taylor's series and substituted into Equation (17):

$$W' = \frac{1}{\Delta Z}\sqrt{\frac{\rho_v}{2\mu a(1-n)X_I t}} \int_{Z_1}^{Z_2} \Delta P^{\frac{1-n}{2}} \left[1 - n\left(\frac{\Delta P_i}{\Delta P}\right)^{1-n}\right]^{1/2} dZ$$

$$= \frac{1}{\Delta Z}\sqrt{\frac{\rho_v}{2\mu a(1-n)X_I t}} \int_{Z_1}^{Z_2} \Delta P^{\frac{1-n}{2}} \left[1 - \frac{n}{2}\left(\frac{\Delta P_i}{\Delta P}\right)^{1-n} - \frac{n^2}{8}\left(\frac{\Delta P_i}{\Delta P}\right)^{2(1-n)} + \ldots\right] dZ$$

$$= \frac{1}{\rho_I g \Delta Z}\sqrt{\frac{\rho_v}{2\mu a(1-n)X_I t}} \int_{\Delta P(Z_1)}^{\Delta P(Z_2)} \Delta P^{\frac{1-n}{2}} \left[1 - \frac{n}{2}\left(\frac{\Delta P_i}{\Delta P}\right)^{1-n} - \frac{n^2}{8}\left(\frac{\Delta P_i}{\Delta P}\right)^{2(1-n)} + \ldots\right] d(\Delta P) \tag{18}$$

By neglecting the third- and higher-order terms, Equation (18) can be integrated:

$$W' = \frac{1}{\rho_I g \Delta Z}\sqrt{\frac{\rho_v}{2\mu a(1-n)X_I t}} \left[\frac{2}{3-n}\Delta P^{\frac{3-n}{2}}(Z) - \frac{n}{1+n}\Delta P_i^{1-n}\Delta P^{\frac{1+n}{2}}(Z)\right]_{\Delta P_0 + \rho_I g Z_1}^{\Delta P_0 + \rho_I g Z_2} \tag{19}$$

The time average filtration flux can be obtained as

$$\overline{W'} = \frac{1}{t_c}\int_0^{t_c} W' dt$$

$$= \frac{2}{\rho_I g \Delta Z}\sqrt{\frac{\rho_v}{2\mu a(1-n)X_I t_c}} \left[\frac{2}{3-n}\Delta P^{\frac{3-n}{2}}(Z) - \frac{n}{1+n}\Delta P_i^{1-n}\Delta P^{\frac{1+n}{2}}(Z)\right]_{\Delta P_0 + \rho_I g Z_1}^{\Delta P_0 + \rho_I g Z_2} \tag{20}$$

The maximum error associated with neglecting the higher-order terms occurs when $\Delta P = \Delta P_i$. This error is 6.0% for $n = 0.5$. It will be shown later that $n = 0.5$ for neutralized acid mine drainage sludge.

Implications of Model

The mathematical model can be used to predict the time average filtration flux over the hose $\overline{W'}$, the differential filtration flux J, the cake thickness l_c, and the amount of dry cake per unit area ω. Examination of Equations (16), (19), and (20) indicates that ln J and ln W' (or ln $\overline{W'}$) should decrease linearly with respect to ln t during filtration. Three empirical parameters exist in the model: ΔP_i, n, and a.

The pressure effect appears in two terms in the model with the exponents $(3 - n)/2$ and $(1 + n)/2$. It is complicated to predict the effect of pressure on filtration rate from the model unless some approximation is made. If $\Delta P >> \Delta P_i$, then the pressure dependence in Equations (16), (19), and (20) would become

$$J = \sqrt{\frac{\rho_v}{2\mu a(1-n)X_I t}}\,\Delta P^{\frac{1-n}{2}} \tag{21}$$

$$W' = \frac{2}{\rho_I g(3-n)\Delta Z}\sqrt{\frac{\rho_v}{2\mu a(1-n)X_I t}} \left[\Delta P^{\frac{1-n}{2}}(Z_2) - \Delta P^{\frac{3-n}{2}}(Z_1)\right] \tag{22}$$

$$\overline{W'} = \frac{4}{\rho_I g(3-n)\Delta Z}\sqrt{\frac{\rho_v}{2\mu a(1-n)X_I t_c}} \left[\Delta P^{\frac{3-n}{2}}(Z_2) - \Delta P^{\frac{3-n}{2}}(Z_1)\right] \tag{23}$$

An inspection of Equation (22) or (23) shows a dependence of filtration rate on the square root of X_I. Therefore, the filtration rate decreases as X_I increases, where X_I is the same as the fraction of undissolved solids in the feed X_ϕ if no settling occurs in region I.

EXPERIMENT

An experimental dual functional filter was constructed that would permit measurement of the filtration rate as a function of axial position along the hose. This system provided experimental data that were used to test the model that was developed above. The capability of measuring the filtration rate as a function of position is critical in view of the fact that the pressure driving force for filtration varies linearly with axial position along the hose.

Equipment

The dual functional filter was constructed from a 3.3 m long porous polypropylene hose (2.8 cm I.D.) installed vertically with on-off valves at the top and bottom of the hose, respectively. Four 4 gal plastic cylinders were mounted along the filter hose as filtrate receiving collars. A 2.5 cm I.D. hole was drilled at the center of each collar to fit the hose. It was designed to be tight enough to avoid leakage of filtate between two collars but not tight enough to reduce the cross section of

the hose at the point of contact. The equipment is illustrated in Figure 4. The filtrate received by the collars was drained to the graduated cylinders for measurement. A stainless steel vessel pressurized with compressed air was used as a feed reservoir.

A conical sludge receiver was employed. This geometry minimizes redispersion of cake particles (region II) into the liquid (region I).

Slurry Feed

All of the dual functional filter performance data presented here were determined with a slurry obtained from neuturalized acid mine drainage water. The acid mine drainage water was neutralized with lime to *p*H 7.5. The particle size distribution of the sludge particles ranged from 2.5 to 5.0 μ. The average particle size was 3.5 μ. The neutralized acid mine drainage sludge was obtained from an EPA Acid Mine Drainage Water Test Site located at Crown, West Virginia. The particle concentrations of these slurries were typically 0.2 wt.%. Several runs were made with clarified sludge which had a particle concentration of approximately 7 wt.%.

Neutralized acid mine drainage sludge provides a critical test of dual functional filter performance. The particles are highly gelatinous due to the presence of iron and aluminum hydroxides. Filter cakes formed from such particles can be expected to be highly compressible and difficult to dewater.

Procedures

The filter has to be filled prior to the beginning of each run. The feed material must be well mixed to obtain a uniform concentration of particles in the pressurized vessel before it is introduced to the filter. Once the hose is filled, the quantity of filtrate from each collar is recorded. Feed was sampled several times during the operation to confirm a constant particle concentration. The valves at both ends of the hose were operated simultaneously at the end of the cycle. The top valve was turned off to shut down the feed to the filter while the bottom valve was opened. This operation produces a pressure shock which caused the hose to collapse. This action discharges the cake and feed liquid from the hose; that is, the unfiltered liquid (region I) and the cake (region II) are collected in a conical receiver and decantation is conducted to recover the concentration sludge. Samples from the unfiltered liquid, cake, and filtrate from each collar were obtained. The particle concentration (undissolved solids) was determined by Millipore (0.45 μ) filtration, drying, and subsequent weighing.

The filter (hose) did not fill instantaneously. In some cases 30 s to 1 min. were required to fill the hose. The start of the run (zero time) was defined as the time at which the hose was full. Consequently, a reference or zero time correction was applied to the data prior to comparing the experimental filtration rate—time dependence with the model. This correction is discussed in a later section.

Variables Investigated

The following variables associated with the performance of the dual functional filter were investigated:

1. Feed pressure 5.5, 43, 74.5, and 123 kN/m^2. The feed pressure is the pressure at the top of the hose.
2. Filtration time: 10 min.
3. Feed concentration 0.2 and 7 wt.% solids (undissolved).

Several potential variables were held constant in this study. These included *p*H of the slurry, the size and configuration of the hose, the material of construction of the hose, and the process temperature which was held at approximately 25° C.

The experimental results are presented in the following section and compared with the mathematical model that was developed for the dual functional filter. The experimental filtration rate—time data were reproducible within ±11% standard deviation.

RESULTS AND DISCUSSION

The filtration rate along the hose, measured with respect to pressure time and feed concentration, is used in conjunction with the model to evaluate the empirical parameters n, a, and ΔP_i. In addition, several effects predicted by the model are tested with experimental data.

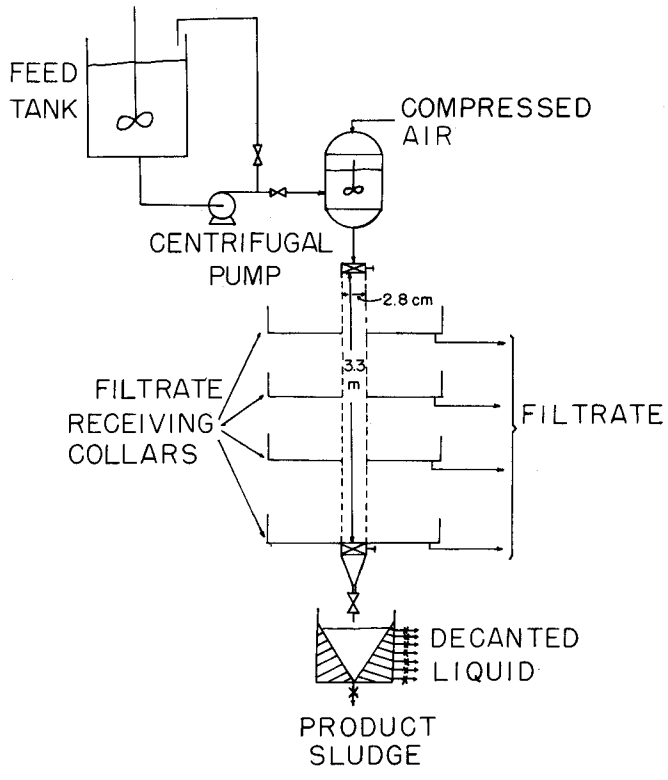

Fig. 4. Experimental dual functional filter.

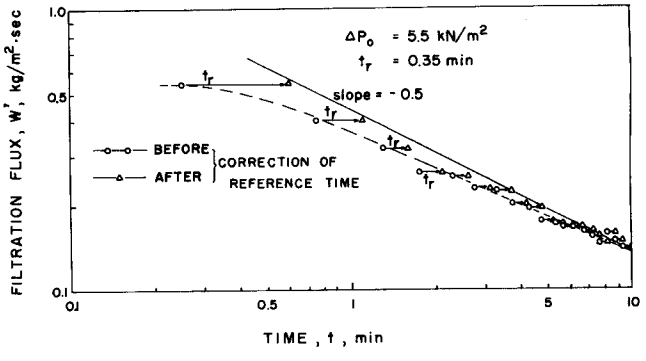

Fig. 5. Filtration flux vs. time with referenced time correction.

The filter performance is controlled by the filtration phase of the cycle. The dump phase of the cycle recovers the cake from the filter hose prior to further concentration by settling. Most of the effort in the experimental investigation was devoted to obtaining the performance of the filtration phase of the cycle. Only the fractional redispersion (f) of solid particles from cake (region II) and the product sludge concentration after settling were measured after the filtration phase of the cycle.

Reference Time Correction in Filtration Phase of the Cycle

The time variable t used in the model has been corrected to include both the fill-up time of the filter hose and the filtration time. The data after correction for reference time give a square-root dependence with time regardless of the operation pressure or feed concentration. An example of this correction is shown in Figure 5.

Evaluation of the Empirical Parameters in the Model

The three empirical parameters n, a, and ΔP_i can be evaluated from Equation (19) and the experimental data. Equation (19) can be written in a form more suitable for regression analysis:

$$W' = K_1 Y_1 + K_2 Y_2 \qquad (24)$$

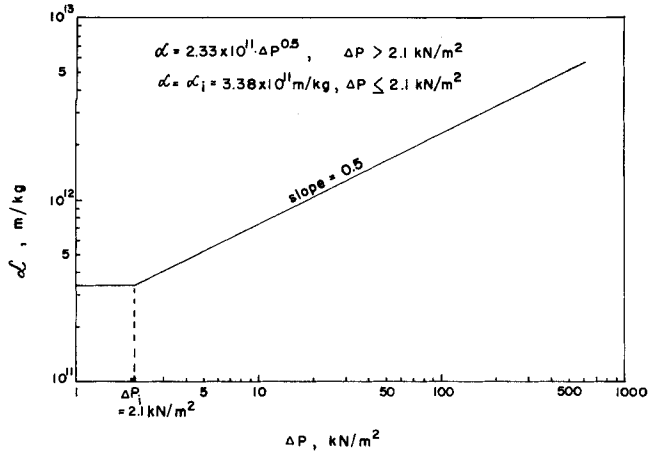

Fig. 6. Specific cake resistance.

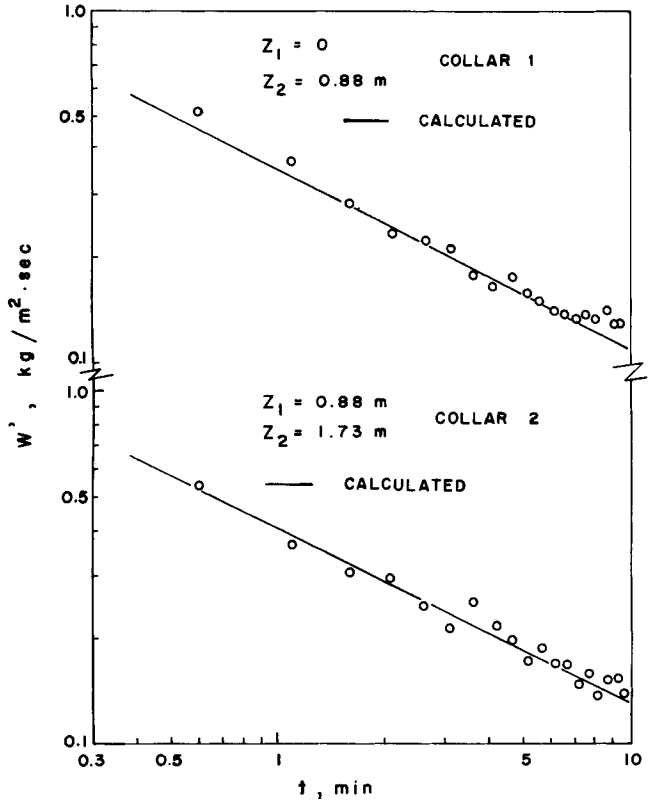

Fig. 7. Filtration flux—time dependence.

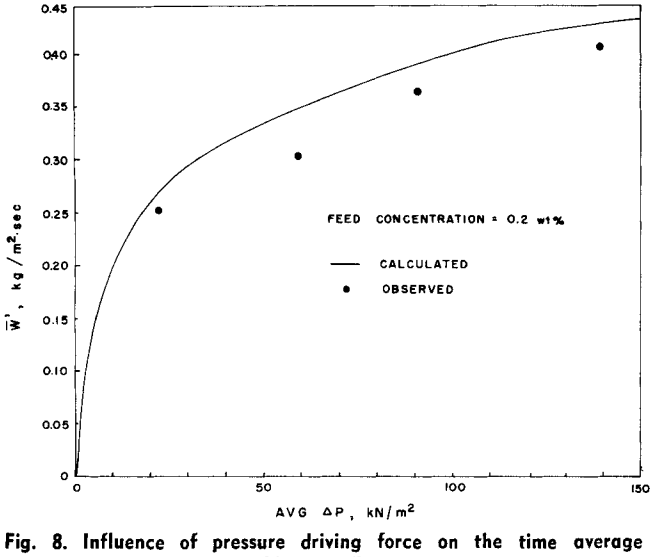

Fig. 8. Influence of pressure driving force on the time average filtration flux.

where

$$K_1 = \frac{2}{\rho_I g(3-n)\Delta Z}\sqrt{\frac{\rho_v}{2a(1-n)\mu X_I}}$$

$$K_2 = -\frac{n}{\rho_I g(1+n)\Delta Z}\Delta P_i^{1-n}\sqrt{\frac{\rho_v}{2a(1-n)\mu X_I}}$$

$$Y_1 = [\overline{\Delta P^{\frac{3-n}{2}}}(Z_2) - \overline{\Delta P^{\frac{3-n}{2}}}(Z_1)]\, t^{-0.5}$$

$$Y_2 = [\overline{\Delta P^{\frac{1+n}{2}}}(Z_2) - \overline{\Delta P^{\frac{1+n}{2}}}(Z_1)]\, t^{-0.5}$$

The filtration flux W' averaged over a portion of hose can be obtained from experiment. Linear plots of W' vs. Y_1 and Y_2 are obtained with slopes of K_1 and K_2, respectively.

Using multiple linear regression with different values of n in Equation (24), one can obtain the value of two empirical parameters a and ΔP_i. Observation of the resulting standard deviations from the regression analysis at different n values indicates that a value of n equal to 0.5 gives the minimum standard deviation. Associated with this specific n value, the other two empirical parameters will have the values of 2.33×10^{11} in metric system for a and 2.1 kN/m² for ΔP_i. Therefore, the expression for specific cake resistance from Equations (3) and (4) becomes

$$\alpha = (2.33 \times 10^{11})\Delta P^{0.5} \quad \Delta P > \Delta P_i \tag{25}$$

$$\alpha = \alpha_i = (2.33 \times 10^{11})\Delta P_i^{0.5} \quad \Delta P \leq \Delta P_i \tag{26}$$

where ΔP and ΔP_i are in kilonewtons per square meters, and α is in meters per kilograms. This relation is shown in Figure 6.

Simplification of the Empirical Model

Expression of specific cake resistance discussed previously includes two forms. When $\Delta P \leq \Delta P_i$, it is a constant α_i; when $\Delta P > \Delta P_i$, it is an exponential function of pressure. The regression value of ΔP_i is 2.1 kN/m². Owing to the fact that pressure at the top of the hose is varied from 5.5 to 123 kN/m², it is reasonable to neglect the term involving ΔP_i [see Equations (19), (20) and (15]. The general model derived previously can then be simplified as follows:

$$W' = \frac{1.66 \times 10^{-6}}{\rho_I g \Delta Z}\sqrt{\frac{\rho_v}{\mu X_I t}}\,[\Delta P^{1.25}(Z_2) - \Delta P^{1.25}(Z_1)] \tag{27}$$

$$\bar{W}' = \frac{3.32 \times 10^{-6}}{\rho_I g \Delta Z}\sqrt{\frac{\rho_v}{\mu X_I t_c}}\,[\Delta P^{1.25}(Z_2) - \Delta P^{1.25}(Z_1)] \tag{28}$$

$$l_c = \frac{4.14 \times 10^{-6}}{X_{II}\rho_{II}}\sqrt{\frac{X_I \rho_v t}{\mu}}\,\Delta P^{0.25}(Z) \tag{29}$$

It is critical to note that the constants in these equations are specific to neutralized acid mine water sludge.

Filtration Rate—Parameter Dependences

The filtration rate decays exponentially with time. The data, ln W' vs. ln t, illustrated in Figure 7 confirm the inverse square-root dependence predicted by the model.

Inspection of the model [Equation (28)] developed previously shows that the pressure dependent term is $[\Delta P^{1.25}(Z_2) - \Delta P^{1.25}(Z_1)]$ for the time average filtration

flux $\overline{W'}$. A plot of $\overline{W'}$ vs. the average pressure applied to the filter is shown in Figure 8. The solid line, calculated from the mathematical model [Equation (28)], is consistent with the experimental data. The time average filtration flux $\overline{W'}$ is a strong function of pressure below 40 kN/m². However, when average pressure is above 40 kN/m², $\overline{W'}$ increases slowly with pressure. The data and model both suggest that moderate filtration pressures should be employed.

The effect of feed concentration on filtration rate is expressed in the term $X_I^{-0.5}$ for the filtration flux $\overline{W'}$ where X_I is approximately equal to the feed concentration. The curve for the higher feed concentration is calculated by assuming that the cake resistance is independent of feed concentration. The model is used with the empirical parameters a and n determined for a feed concentration of 0.2 wt.%. These data are essentially extrapolated for a feed of 7 wt.% by increasing the value of X_I. The agreement between the data and model for the 7 wt. % feed as shown in Figure 9 is excellent; that is, the average deviation between experimental and predicted filtration rates is ±15%.

Physically, the large decrease in filtration rate with feed concentration can be explained by the fact that thicker cakes are formed with the higher feed concentrations. The material balance effect is represented by $(X_I)^{-0.5}$ in the model.

Calculated Cake Thickness

Cake thickness profiles are calculated to evaluate the assumption that the cake thickness is much smaller than the hose diameter. Equation (29) is used to calculate the cake thickness.

The cake thickness l_c increases with time as shown in Figure 10. The calculated thickness is 0.14 cm at a position 1.86 m from the hose inlet after 10 min. at an inlet pressure of 5.5 kN/m². Comparatively, its thickness is 0.17 cm for an inlet pressure of 123 kN/m². Both of these values are much less than the diameter of the hose which is 2.8 cm I.D. This supports the assumption that $l_c << 2R$. Figure 11 shows the profile of cake thickness along the filter for inlet pressures of 5.5 and 123 kN/m². The cake thickness is a stronger function of position at low hose inlet pressure than high pressure. This is due to the fact that the hydrostatic contribution to the pressure is greater when the inlet pressure is small, that is, there is significant pressure variation with position.

Predictive Capability of the Model

The model can be used to predict the average filtration flux for the entire hose. The time average filtration flux over the filtration phase of the cycle is calculated from Equation (28). The minimum and maximum deviations of the predicted filtration rates from the experimental values are 6 and 15%, respectively. This is acceptable agreement in view of the fact that the filtration data were obtained with different samples of neutralized acid mine drainage sludge.

The dual functional filter model includes the effects of the axial variation of the pressure driving force. Calculations with this model are compared with the batch filtration equation. This is accomplished by utilizing the average filtration pressure in the conventional batch filtration equation [see Equation (30)]:

$$\overline{W'} = \sqrt{\frac{4\rho_v}{aX_I\mu t_c}}\,\overline{\Delta P_{\text{avg}}^{\frac{1-n}{2}}}\,(Z) \qquad (30)$$

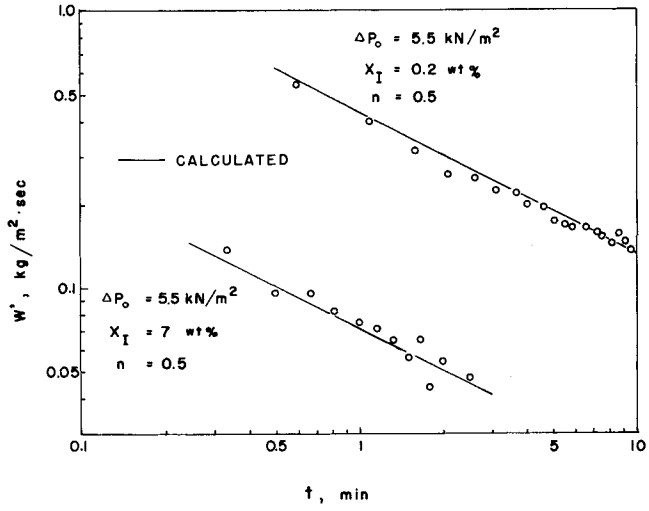

Fig. 9. Influence of feed concentration on filter performance.

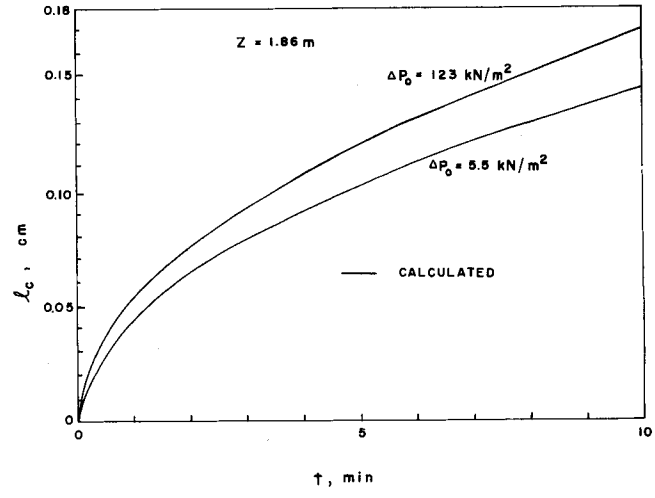

Fig. 10. Filter cake thickness.

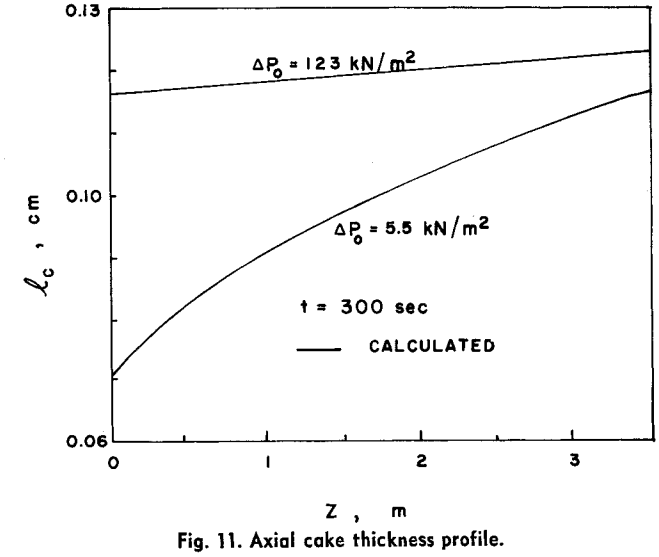

Fig. 11. Axial cake thickness profile.

where $\Delta P_{\text{avg}} = [\Delta P(Z_2) + \Delta P(Z_1)]/2$. This expression assumes that $\rho_v \simeq \rho_I$.

Figure 12 illustrates the errors that are obtained by applying the batch filtration equation rather than the model which includes a varying pressure driving force. The errors are illustrated as a function of n, the exponent in the specific resistance-pressure dependence. Note that

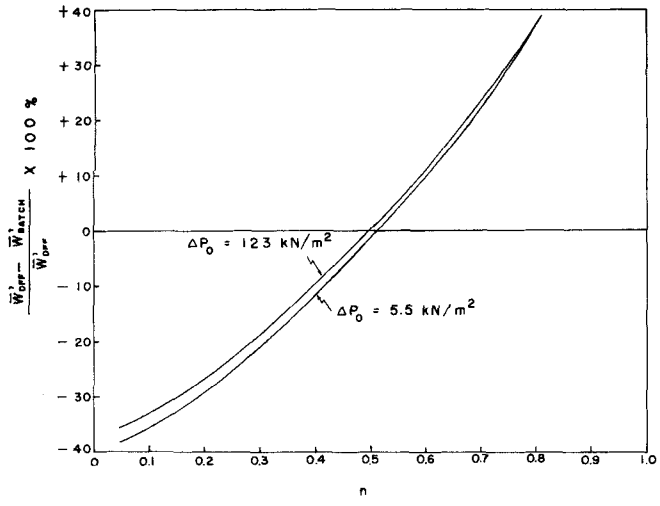

Fig. 12. Comparison of filtration fluxes predicted by the dual functional filter model and constant pressure batch filtration equation.

fortuitously with an n value of 0.5 for the neutralized acid mine sludge, the filtration rates calculated by the batch equation and the dual functional filter model are the same. This will not be the case with slurries which have different n values. Figure 12 indicates, for example, that the batch equation would underpredict the filtration rate by 37% at an n value of 0.8.

Performance of the Dump and Settling Phases of the Cycle

Filter cake and feed liquid are dumped from the hose at the end of the filtration phase. This heterogeneous mixture is settled prior to decantation to recover the concentrated product sludge. The pressure shock associated with relaxing the pressure in the hose is the driving force for ejecting the cake from the hose. Material is dumped from both regions I and II of the hose.

Ideally, none of the cake particles from region II would redisperse into the interior core of feed liquid that is region I. Experimental data indicate that some of the particles from region II do redisperse into the region I liquid. This partial redispersion of the filter cake leads to a decanted liquid that has a higher particle concentration than the original feed. Owing to the fact that the decanted liquid is recycled to the feed tank, the effective feed concentration to the filter is higher than the original external feed.

The effect of the redispersion of the filter cake on the feed concentration can be illustrated by material balance. If f is defined as the fraction of the solids in the filter cake that are redispersed during the dump phase of the cycle into the region I liquid, then a material balance indicates that the actual feed concentration to the hose is higher than the external feed concentration. This effect is summarized by the following material balance equation:

$$X_\phi = \frac{X_F}{1-f} \tag{31}$$

X_ϕ is the actual concentration fed to the hose, X_F is the external feed concentration, and f is the fractional redispersion. Note that when $f = 0$ (no redispersion), the internal feed concentration is the same as the feed concentration.

The dependence of the internal feed concentration on the performance of the dump phase of the cycle provides an opportunity to emphasize the coupling that occurs between the dump and filtration phases. The solids concentration in region I, X_I, is equal to the internal rather than the external feed concentration. Note that X_I must be specified in the equations which are used to calculate filtration rate. It has been experimentally confirmed that X_I is essentially the same as the actual feed concentration to the hose, X_ϕ.

Table 1. Redispersion of the Filter Cake During the Dump Phase of the Cycle

Average pressure, kN/m²	Feed concentration, wt. %	Redispersion, f, %
22	0.2	41
59	0.23	47
91	0.19	35
140	0.17	20

The fractional redispersion of the filter cake can be measured as a function of the average filtration pressure. Table 1 illustrates these data. The fractional redispersion decreases with increasing filtration pressure. This may be due to the compressible nature of the filtration cake; that is, the particles are more consolidated in the cake at higher pressures and thus tend to redisperse to a lesser extent into the region I liquid. The fractional redispersion should be 20% or less at the higher pressures that would be selected for filter operation.

The dump and settling phases of the cycle produce sludges of very high solids content. Product sludge concentration of 20 to 35 wt.% can be obtained from feed material which has a solids content of 0.2 wt.%. This represents an extremely effective sludge dewatering in view of the gelatinous nature of the sludge particles.

Potential Applications of the Dual Functional Filter

The dual functional filter is a novel solid-liquid separation device which has not been utilized commercially. It has several important advantages which can be considered when selecting a solid-liquid separation process: very high degrees of sludge dewatering, high filtration rates, and mechanical simplicity. The neutralized acid mine drainage sludge system provides a severe test of filter performance. Generally, this filter should find application for dewatering a variety of sludges which are difficult to dewater by conventional techniques.

Both the mathematical model and the experimental evaluation procedure should be useful in evaluating both pilot and commercial scale filter performance.

ACKNOWLEDGMENT

The authors express their appreciation to the National Science Foundation (Grant GK 42082) and the West Virginia Water Research Institute for partial support of this research. Portions of the experimental equipment were provided by the Environmental Protection Agency and Continental Oil Company. Dr. Frank Tiller provided many suggestions and constructive criticisms which strengthened this work.

NOTATION

a = constant defined in Equations (3) and (4)
f = fractional redispersion, dimensionless
g = gravitational acceleration, 9.8 m/s²
J = mass flux of filtrate at R, kg/m² · s
l_c = cake thickness, m
n = compressibility factor, dimensionless
N = mass flux of filtrate at r, kg/m² · s
ΔP = pressure difference between the flow inside the filter hose and the atmospheric pressure, kN/m²
ΔP_0 = ΔP at the top of the filter hose, kN/m²
ΔP_i = critical pressure defined in Equations (3) and (4), kN/m²

Q = mass flow rate in axial direction inside the filter hose, kg/s
r = radial distance from center of the filter hose to the surface of cake, m
R = radius of the filter hose, m
R_m = filter medium resistance, m^{-1}
t = time, s
t_c = cycle time, s
ω = amount of dry cake per area, kg/m^2
W' = average mass flux (or rate) of filtrate from a segment of the hose between filtrate collars, kg/m^2 · s
$\overline{W'}$ = time average filtration flux over a segment of hose, kg/m^2 · s
X = weight fraction of solid particle in slurry, dimensionless
Z = axial distance along the filter hose, m
α = specific cake resistance, m/kg
α_i = constant specific cake resistance when $\Delta P \leq \Delta P_i$, m/kg
μ = viscosity, kN · s/m^2
ρ = density, kg/m^3

Subscripts

avg = average
DFF = dual functional filtration
v = filtrate
I = region I (slurry phase)
II = region II (cake phase)
F = external feed concentration
ϕ = actual feed concentration fed to the hose

LITERATURE CITED

Holland, C. D., and J. F. Woodham, "Continuous Vacuum Rotary Filters," *Petrol. Refiner*, 35, No. 2, 149 (1956).

Lui, A. P., "Dewatering of Neutralized Acid Mine Sludge With a Dual Functional Filter," M.S. thesis, West Va. Univ., Morgantown (1974).

Nawrocki, M. A. (Hittman Associates, Inc.), "Demonstration of the Separation and Disposal of Concentrated Sediments," *Contract No. 68-01-0743*, Office of Research and Development, U.S. Enivronmental Protection Agency (June, 1974).

Page, B. W., M. J. Copely, and J. M. Shackelford, "A New Filtration Device for Concentrating Neutralized AMD Sludge," *The Fourth Symposium on Coal Mine Drainage*, Pittsburgh, Pa. (Apr., 1972).

Popper, K., and W. M. Camirand, "Uni-Flow Filter and Method," *U.S. Patent 3,523,077* (1970).

Ruth, B. F., "Correlating Filtration Theory With Industrial Practice," *Ind. Eng. Chem.*, 38, 564 (1946).

Tiller, F. M., and H. Cooper, "The Role of Porosity in Filtration, Part V: Porosity Variation in Filter Cakes, *AIChE J.*, 8, 445-449 (1962).

Tiller, F. M., "Rotary Drum Filtration—Part I: Incompressible Cakes with Hydrostatic Head," *Filtration and Separation*, 9, 60-64 (1972).

Manuscript received October 21, 1974; revision received December 1, 1975 and accepted December 4, 1975.

Onset of Draw Resonance During Isothermal Melt Spinning: A Comparison Between Measurements and Predictions

C. B. WEINBERGER
G. F. CRUZ-SAENZ
and
G. J. DONNELLY

Department of Chemical Engineering
Drexel University
Philadelphia, Pennsylvania 19104

Various polymer melts were spun isothermally to determine the critical extensional strain at which draw resonance occurs. Simultaneously, the variation of apparent spinning viscosity with extensional strain was measured. Experimental results failed to confirm the theoretical prediction that strain thickening behavior leads to enhanced stability.

SCOPE

The phenomenon of draw resonance is of significant importance in polymer processing. Such resonance appears as a cyclic pulsation in extrudate thickness as polymeric material is continuously extruded and drawn, for example, film coating, fiber spinning, etc. The pulsation, although constant in terms of thickness amplitudes for fixed extrusion and take-up speeds, becomes more severe as take-up speed is increased.

The dynamics of typical drawing operations can frequently be expressed in terms of tensile force which is constant with respect to position but variable with respect to time. Such dynamics obtain when the viscosity is sufficiently large to render negligible the contributions from gravity, inertia, and surface tension to the tensile force. For these dynamics, linearized perturbation analyses (Kase et al., 1966; Pearson and Matovich, 1969; Gelder, 1971) of the spinning of Newtonian fluids have shown that the onset of such resonance occurs at a critical draw ratio, E_{crit} = take-up speed/extrusion speed at onset, of about 20. This theoretical result has recently been corroborated by spinning experiments with a Newtonian silicone oil (Donnelly and Weinberger, 1975). For the constant-

G. F. Cruz-Saenz and G. J. Donnelly are with E. I. du Pont de Nemours, Inc., Wilmington, Delaware.